

PATTERN FORMATION IN A STOCHASTIC MODEL OF CANCER GROWTH

ANNA OCHAB-MARCINEK

Marian Smoluchowski Institute of Physics, Jagellonian University
Reymonta 4, 30-059 Kraków, Poland

(Received February 10, 2005)

We investigate noise-induced pattern formation in a model of cancer growth based on Michaelis–Menten kinetics, subject to additive and multiplicative noises. We analyse stability properties of the system and discuss the role of diffusion and noises in the system’s dynamics. We find that random dichotomous fluctuations in the immune response intensity along with Gaussian environmental noise lead to emergence of a spatial pattern of two phases, in which cancer cells, or, respectively, immune cells predominate.

PACS numbers: 05.40.–a, 87.10.+e, 89.75.Kd

1. Introduction

The study of population dynamics covers a wide range of fields such as ecology, cellular and molecular biology and medicine (see *e.g.* [1–4]). The models of population growth based on nonlinear ordinary differential equations, despite their simplicity, can often capture the essence of complex biological interactions and explain characteristics of proliferation phenomena. However, biological processes are not purely deterministic: systems existing in nature are subject to natural noises.

The presence of noise in biological systems gives rise to a rich variety of dynamical effects. Random fluctuations may be regarded not only as a mere source of disorder but also as a factor which introduces positive and organising rather than disruptive changes in the system’s dynamics. Some of the more important examples of noise induced effects are stochastic resonance [2, 5], resonant activation [6–8], noise-induced transitions [9, 10], noise-enhanced stability [11] and pattern formation [1, 2, 12].

The effect of cell-mediated immune surveillance against cancer [13–15] may be a specific illustration of the coupling between noise and a biological system. Most of tumoral cells bear antigens which are recognised as strange by the immune system. A response against these antigens may be mediated

either by immune cells such as T-lymphocytes or other cells, not directly related to the immune system (like macrophages or natural killer cells). The process of damage to tumour proceeds via infiltration of the latter by the specialised cells which subsequently develop a cytotoxic activity against the cancer cell-population. The series of reactions between the cytotoxic cells and the tumour tissue may be considered to be well approximated by a saturating, enzymatic-like process whose time evolution equations are similar to the standard Michaelis–Menten kinetics [13, 16]. Random variability of kinetic parameters defining that process may effect the extinction of the tumour.

In our previous article [8] we discussed the noise-induced effect of resonant activation in a spatially homogeneous model of cancer growth [16] based upon the above-mentioned kinetic scheme. In the present paper, we focus on the study of a spatially inhomogeneous system, namely, we investigate how global environmental noise as well as fluctuations in the immune response parameter effect the emergence of spatial patterns.

2. The model

The interaction between cancer cells and cytotoxic cells will be described by use of the predator-prey model based upon the Michaelis–Menten kinetic scheme [8, 9, 13, 16–18]. This model is a classical one and has been extensively studied since the 1970s. Its validity has been verified experimentally *e.g.* in [19], where the authors examined the mechanism of immune rejection of a tumour induced by Moloney murine sarcoma virus. The behaviour of the cellular populations may be represented by the following scheme:

First, the cytotoxic cells bind to the tumour cells at rate k_1 ; subsequently, the cancer cells which have been bound are killed and the complex dissociates at rate k_2 ; finally, dead cancer cells decay at a rate k_3 . The process can be described schematically:



X represents here the population of tumour cells. Y , Z and P are populations of active cytotoxic cells, bound cells and dead tumour cells, respectively. Following the original presentation [16], we assume that *(i)* cancer cells undergo replication at a rate proportional to a time constant λ ; *(ii)* as a result of cellular replication in limited volume, a diffusive propagation of cancer cells is possible, with a transport coefficient proportional to the replication rate and local density of cancer cells; *(iii)* dead cancer cells undergo elimination at rate k_3 ; *(iv)* free cytotoxic cells can move with a “diffusion” coefficient D . The spatio-temporal evolution of the tumour due to the above

processes can be then described by a set of balance equations:

$$\begin{cases} \frac{\partial x}{\partial t} &= \lambda[1 - (x + p)]x - k_1yx + \lambda(1 - p)\nabla^2x + \lambda x\nabla^2p, \\ \frac{\partial y}{\partial t} &= -k_1yx + k_2z + D\nabla^2y, \\ \frac{\partial z}{\partial t} &= k_1yx - k_2z, \\ \frac{\partial p}{\partial t} &= k_2z - k_3p. \end{cases} \quad (2)$$

The $x(\vec{r}, t), y(\vec{r}, t), z(\vec{r}, t)$ and $p(\vec{r}, t)$ are local densities of cells at point \vec{r} . Finally, we impose an additional condition on the model: the total number of active and bound cytotoxic cells should remain constant:

$$y(t) + z(t) = \text{const.} = E. \quad (3)$$

Below, we analyse several versions of the model:

- Bifurcation analysis, based on a bare kinetics model without spatial diffusion (Sec. 4.1)
- Incorporation of Fickian diffusion terms in evolution equations for $x(\vec{r}, t), p(\vec{r}, t)$ respectively, which leads to a wavefront solution (Sec. 4.2).
- We determine the effect of the dichotomous switching in the kinetic parameter k_1 and discuss its role also for the model system in which each of the kinetic equations is additionally driven by a Gaussian noise term of the same intensity (Sec. 4.3, 4.4, 4.5).
- At the last step of the model complexity, we analyse how the joint effect of diffusion, additive Gaussian fluctuations and independent dichotomic switching in k_1 parameter affect the cancer cells population dynamics (Sec. 4.6).

3. Simulation

The basic aim of this work was to study the behaviour of the system (2) subject to additive and multiplicative noises:

$$\begin{cases} \frac{\partial x}{\partial t} &= \lambda[1 - (x + p)]x - (k_1 + \eta(t))yx \\ &\quad + \lambda(1 - p)\nabla^2x + \lambda x\nabla^2p + \sigma\xi(\vec{r}, t), \\ \frac{\partial y}{\partial t} &= -(k_1 + \eta(t))yx + k_2z + D\nabla^2y + \sigma\xi(\vec{r}, t), \\ \frac{\partial z}{\partial t} &= (k_1 + \eta(t))yx - k_2z + \sigma\xi(\vec{r}, t), \\ \frac{\partial p}{\partial t} &= k_2z - k_3p + \sigma\xi(\vec{r}, t). \end{cases} \quad (4)$$

The multiplicative dichotomous Markovian noise $\eta(t) = \pm\Delta$ with mean frequency γ and autocorrelation $\langle\eta(t)\eta(t')\rangle = \frac{\Delta^2}{2}e^{-2\gamma|t-t'|}$ models fluctuations in immune response. The additive Gaussian noise $\xi(\vec{r}, t)$ with autocorrelation $\langle\xi(\vec{r}, t)\xi(\vec{r}', t')\rangle = \delta(\vec{r} - \vec{r}')\delta(t - t')$ depicts external environmental fluctuations. We assume that its intensity σ is same for each variable of the system. Both noises are assumed to be statistically independent: $\langle\xi(\vec{r}, t)\eta(s)\rangle = 0$.

3.1. Numerics

We have solved the stochastic differential equations (4) numerically, using the Euler scheme, on a 128×128 square lattice. According to the statistical properties of $\eta(t)$, the waiting time between two switchings was generated from the exponential distribution.

Since x, y, z and p are densities, their values never can be greater than 1 or less than 0. Consequently, following boundary conditions have been imposed on the simulated system: if x, y, z or p becomes less than 0 or greater than 1 at a given time step, we adjust its value to 0 or to 1, respectively.

3.2. Simulation results

We performed a simulation with the following values of parameters:

$$\begin{aligned} \lambda &= 0.5, & D &= 0.05, & \sigma &= 0.01, & \Delta &= 0.5, \\ k_1 &= 1.75, & k_2 &= 0.1, & k_3 &= 0.1, & \gamma &= 0.01. \end{aligned} \quad (5)$$

γ is the mean rate of switching in $\eta(t)$. Initial conditions:

$$x(\vec{r}, 0) = 0, \quad y(\vec{r}, 0) = 0.4, \quad z(\vec{r}, 0) = 0, \quad p(\vec{r}, 0) = 0. \quad (6)$$

The values of parameters and initial conditions have been chosen so that we could obtain a distinct pattern: The immune response rates $k_1 + \Delta$ and $k_1 - \Delta$, along with λ lead to two different types of stationary behaviour (see Sec. 4.5). The mean switching rate is one or two orders of magnitude slower than other kinetic parameters, which gives the system a possibility to approach the stationary states. The environmental noise intensity σ has been chosen in such a way that it allows the system to jump between both mentioned states. The noise is, however, weak enough to let the system form a pattern. At the selected value of D , the pattern has sufficiently distinct boundaries and is relatively stable (at higher values of D it would dissolve quickly, whereas at smaller D it would form small ‘‘grains’’). Parameters k_2 and k_3 have been chosen by a trial-and-error procedure: k_2 is responsible for the dissociation of z into $y + p$. If the dissociation rate is large, then

the active immune cells y are being released faster and thus the immune response is more effective. The k_3 parameter determines the rate at which dead cancer cells are eliminated. Since dead cells occupy the living space, this parameter controls the effective replication rate of cancer cells.

The simulation results are presented in Fig. 1. After some time, we observe the emergence of the “ y -phase” islands (where the immune cells y predominate) within the relatively homogeneous “ x -phase” (in this phase cancer cells x prevail). The phase boundaries move back and forth depending on the dichotomous changes in the immune response intensity $k_1 \pm \Delta$.

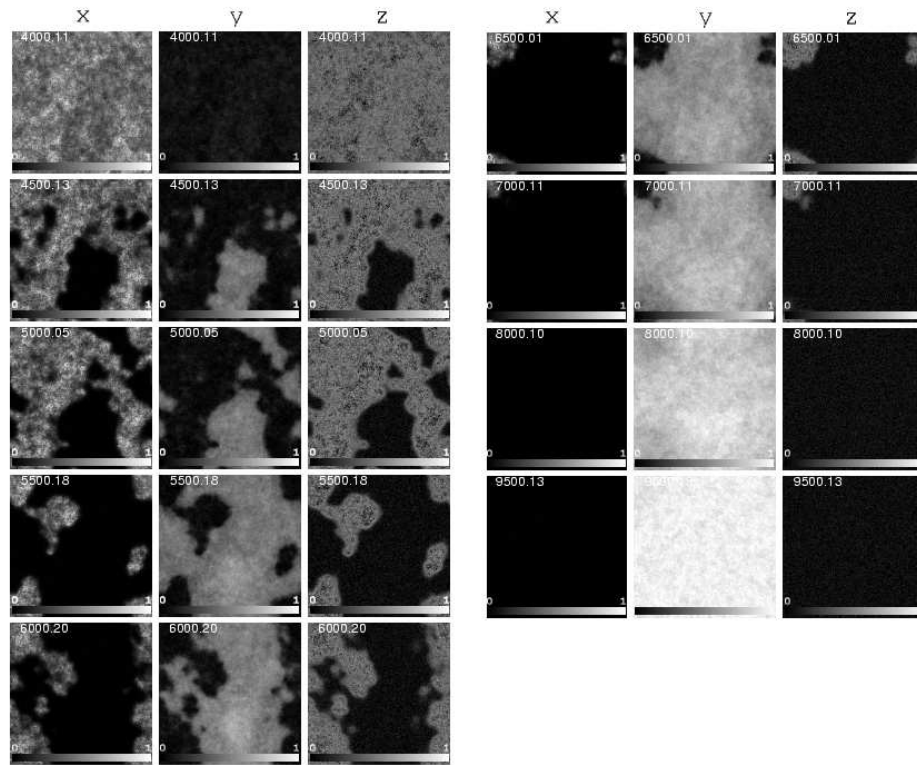


Fig. 1. Snapshots from the simulation of the system (4). Time evolution of the spatial distribution of x , y and z . Time counter in upper left corner of each image. Simulation time $T = 10000$. Initial conditions: $x = 0$, $y = 0.4$, $z = 0$, $p = 0$ everywhere. Parameters: $\lambda = 0.5$, $D = 0.05$, $\sigma = 0.01$, $\Delta = 0.5$, $k_1 = 1.75$, $k_2 = 0.1$, $k_3 = 0.1$, $\gamma = 0.01$. Light pixels: high concentration, dark pixels: low concentration of cells.

4. Analysis

In order to explain the behaviour of the simulated system, we will analyse its stability properties as well as the role of diffusion, additive noise and dichotomous noise in the k_1 parameter.

4.1. Stability analysis

The stationary points $\{x^*, y^*, z^*, p^*\}$ of the system are given by:

$$\{0, y^*, 0, 0\} \tag{7}$$

and

$$\left\{ \frac{k_3}{\lambda} \frac{\lambda - k_1 y^*}{k_3 + k_1 y^*}, y^*, \frac{k_1 k_3 y^*}{\lambda k_2} \frac{\lambda - k_1 y^*}{k_3 + k_1 y^*}, \frac{k_1 y^*}{\lambda} \frac{\lambda - k_1 y^*}{k_3 + k_1 y^*} \right\}. \tag{8}$$

According to (2), the value of y^* is arbitrary. However, if the condition (3) is involved, it defines the value of y^* :

$$y^* + z^* = \text{const.} = E. \tag{9}$$

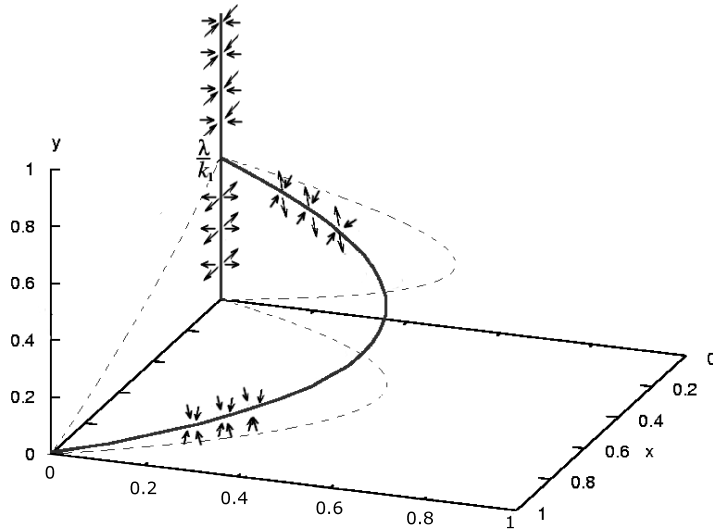


Fig. 2. Sets of stationary points (7), (8) and their stability (shown only schematically by arrows), x - y - z -projection. Dashed lines: planar projections of the curve. Parameters: $\lambda = 0.5$, $k_1 = 1.25$, $k_2 = 0.1$, $k_3 = 0.1$.

The sets of stationary points form two branches in the x - y - z - p -space. The branch (7) changes its stability at the point $\{0, \frac{\lambda}{k_1}, 0, 0\}$. It is repelling for $0 < y < \frac{\lambda}{k_1}$ and attracting for $\frac{\lambda}{k_1} < y < 1$. The branch (8) is attracting for $0 < y < \frac{k_3}{k_1} \left(-1 + \sqrt{1 + \frac{\lambda}{k_1}}\right)$. For $\frac{k_3}{k_1} \left(-1 + \sqrt{1 + \frac{\lambda}{k_1}}\right) < y < 1$ it consists of saddle points.

Trajectories of the deterministic system can lie only on the plane (3), given by the initial conditions for y and z . Hence, the stationary points of such a system lie on the intersection of the plane (3) and the branches (7), (8). Depending on the values of parameters and initial conditions, the system can have 1 (attracting), 2 (attracting and repelling) or 3 (attracting, saddle and attracting) stationary points (see Figs. 2, 3).

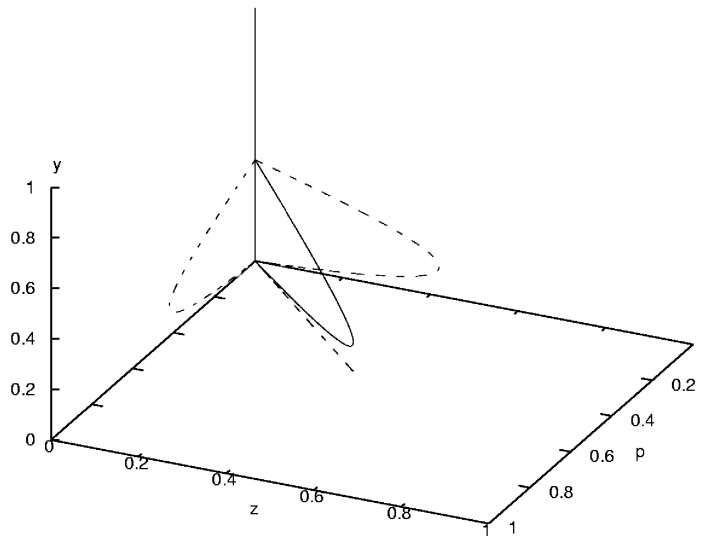


Fig. 3. Sets of stationary points (7), (8) in y - z - p -projection. Dashed lines: planar projections of the curve. Parameters: $\lambda = 0.5$, $k_1 = 1.25$, $k_2 = 0.1$, $k_3 = 0.1$.

When E, k_2, k_3 are fixed, the stability properties of the system depend on the k_1 parameter (see Fig. 4), *i.e.* the immune response efficiency, which, in our simulation, was controlled by the dichotomous noise.

In the next subsections, we will analyse how the presence of noises and diffusion affects the behaviour of the system.

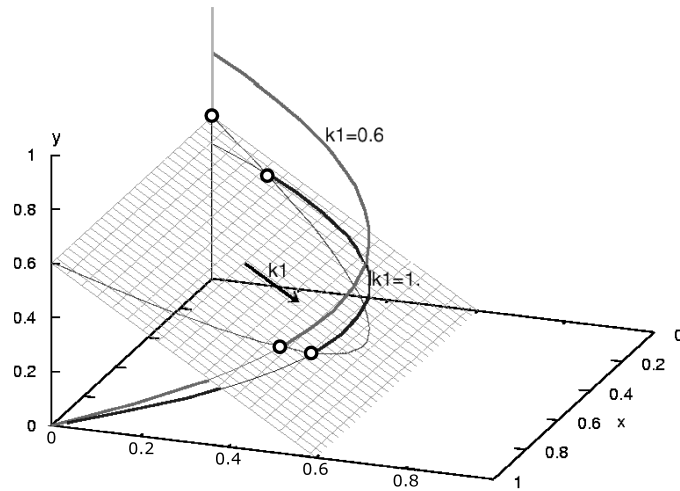


Fig. 4. Stationary points (open circles) lie on the intersection of the plane $y + z = E$ and the curves given by (7), (8). As k_1 grows, the number of intersections changes from 2 to 3 and, subsequently, from 3 to 1. (An arrow shows schematically the direction in which the intersection points move as k_1 grows.) The values of the remaining parameters are here: $E = 0.6$, $\lambda = 0.6$, $k_2 = 0.1$, $k_3 = 0.1$.

4.2. Spatially inhomogeneous system without noise

The solutions to the deterministic system with diffusive terms have the form of travelling wavefronts [20].

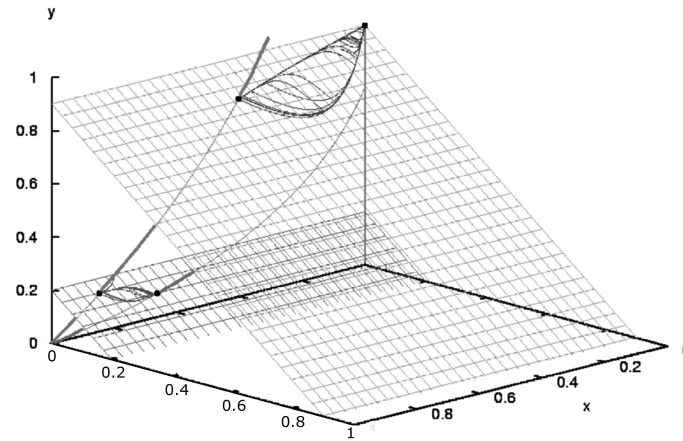


Fig. 5. Example trajectories of the system with dichotomous noise only, for two different values of $E = y + z$: $E = 0.9$ and $E = 0.2$. Parameters: $\lambda = 0.5$, $\gamma = 0.05$, $k_1 = 0.5$, $\Delta = 0.25$, $k_2 = 1$, $k_3 = 1$. Simulation time $T = 700$.

4.3. Spatially homogeneous system with dichotomous multiplicative noise

After the introduction of the dichotomous noise $\eta(t) = \pm\Delta$ into the k_1 parameter, trajectories of the system lie on the planes $y + z = E$ and wander between two stationary points according to the current value of $k_1 \pm \Delta$ (see Fig. 5).

4.4. Spatially homogeneous system with dichotomous multiplicative noise and additive Gaussian white noise

In the next step of complexity, we add the term $\sigma\xi(\vec{r}, t)$ (Gaussian white noise) to each equation, assuming that the additive noise acts in the same way on each variable of the system. Here, the trajectories do not stay on constant planes $y + z = E$ any more. Due to the additive noise, they “slip off” from their initial planes (see Figs. 6, 7).

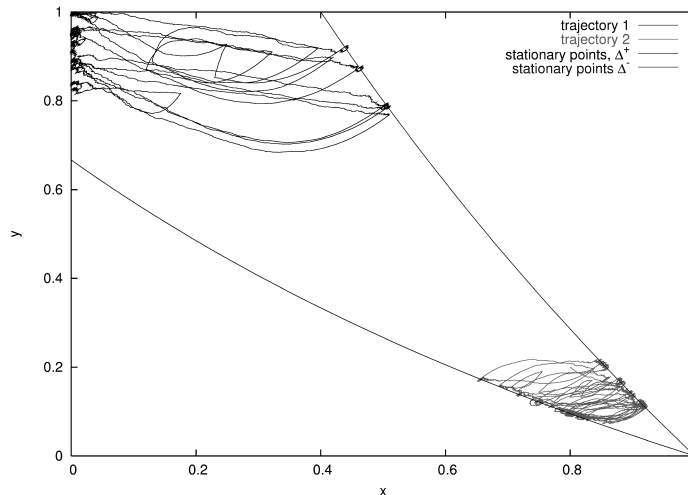


Fig. 6. Two example trajectories of the spatially homogeneous system with multiplicative dichotomous noise, with additive Gaussian noise, starting from two different initial conditions: $y + z = E = 0.9$ and $y + z = E = 0.2$, in x - y -projection. $\sigma = 0.002$, other parameters same as in Fig. 5. To compare with the trajectories without additive noise, see Fig. 5.

4.5. System with Gaussian noise and diffusion

Let us examine a system with the additive Gaussian noise and diffusion, but without the dichotomous noise. Instead, we will take into consideration two situations where the intensity of the immune response is constant:

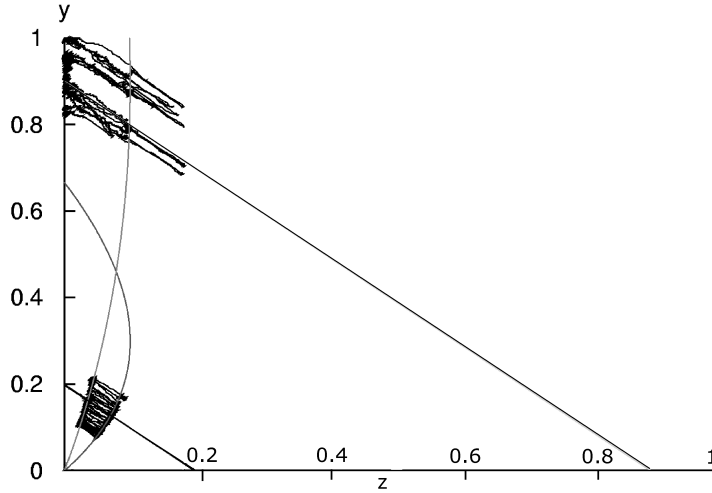


Fig. 7. Two example trajectories of the spatially homogeneous system with multiplicatively dichotomous noise and additive Gaussian noise, starting with two different initial conditions: $E = 0.9$ and $E = 0.2$, in y - z -projection. The trajectories do not stay on their initial planes E (denoted by sloped lines), but move up or down due to the Gaussian noise. Curves: branches of stationary points for switching value of $k_1 \pm \Delta$. $\sigma = 0.002$, other parameters the same as in Fig. 5.

$$K_1 = k_1 - \Delta \quad (10)$$

and

$$K_1 = k_1 + \Delta. \quad (11)$$

The value of Δ is the same as in the first simulation (Sec. 3.2), *i.e.* it corresponds to one of the dichotomous noise states.

For $K_1 = k_1 - \Delta$, the “ x -phase” is more stable. The trajectory starts with initial conditions (6) which is exactly the point $\{0, \frac{\lambda}{k_1}, 0, 0\}$ where two branches of stationary points cross. It is then very likely that the trajectory falls down onto the lower branch of the attractor and stays in its neighbourhood (see Figs. 9, 10).

For $K_1 = k_1 + \Delta$, the “ y -phase” is more stable. Starting far away from the lower branch of the attractor, the trajectory remains close to the upper branch. Moreover, it climbs higher and higher because of the reflecting boundary at $x = 0, y = 0, z = 0, p = 0, x = 1, y = 1, z = 1, p = 1$ (see Figs. 11, 12). This condition imposed on the boundaries is justified by the requirement that the population density cannot be negative nor greater than 1.

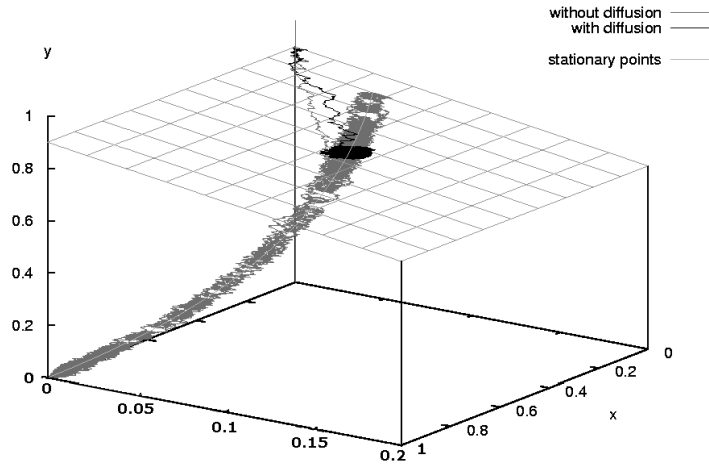


Fig. 8. Stabilising effect of diffusion. Gray: trajectory of a system with diffusion ($D = 0.5$) and additive Gaussian noise, recorded at point $[20, 20]$ on the spatial lattice. Black: trajectory of a system with additive Gaussian noise, but without diffusion ($D = 0$). Parameters: $\lambda = 0.5$, $\sigma = 0.005$, $k_1 = 0.25$, $k_2 = 1$, $k_3 = 1$. Simulation time $T = 3000$.

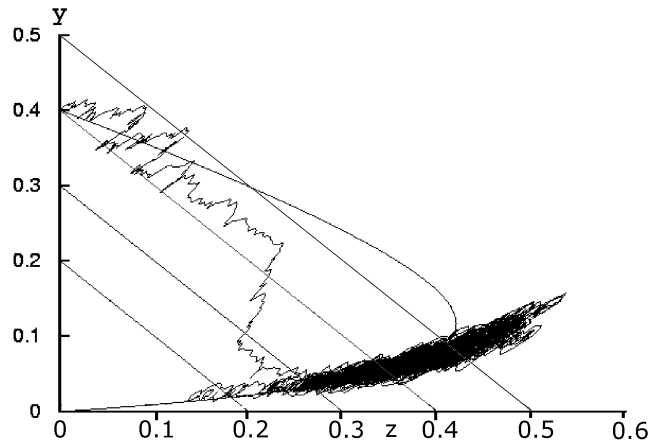


Fig. 9. An example trajectory of the system with additive Gaussian noise and diffusion, recorded at point $[20, 20]$ on the spatial lattice. The immune response parameter $K_1 = k_1 - \Delta = 1.25$. The trajectory falls down onto the “ x -phase” attractor. $\lambda = 0.5$, $D = 0.05$, $\sigma = 0.01$, $\Delta = 0$, $k_2 = 0.1$, $k_3 = 0.1$. Initial conditions: $x = 0$, $y = 0.4$, $z = 0$, $p = 0$. Straight lines: the profiles of example E planes.

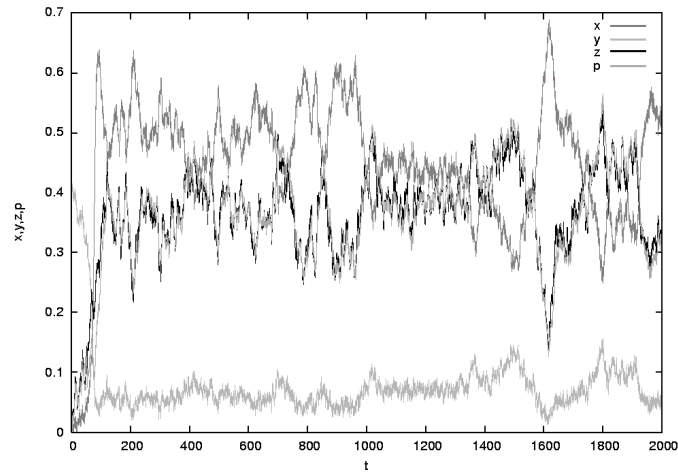


Fig. 10. Time-evolution of x, y, z and p in the system with additive Gaussian noise and diffusion, recorded at point $[20, 20]$ on the spatial lattice. $K_1 = k_1 - \Delta = 1.25$, $\lambda = 0.5$, $D = 0.05$, $\sigma = 0.01$, $\Delta = 0$, $k_2 = 0.1$, $k_3 = 0.1$. Initial conditions: $x = 0$, $y = 0.4$, $z = 0$, $p = 0$.

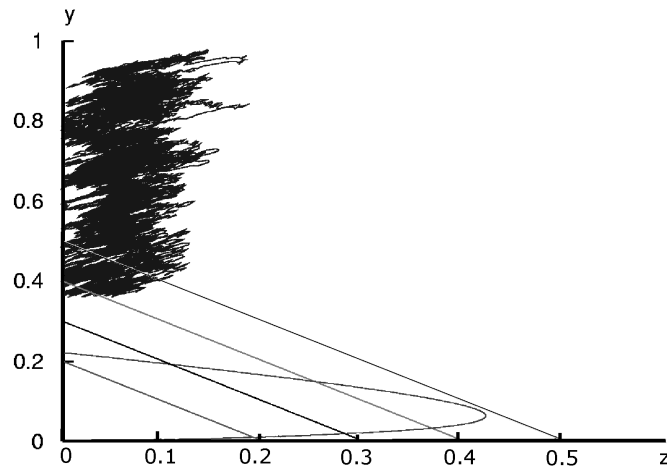


Fig. 11. An example trajectory of the system with additive Gaussian noise and diffusion, recorded at point $[20, 20]$ on the spatial lattice. The immune response parameter $K_1 = k_1 + \Delta = 2.25$. The trajectory remains in the neighbourhood of the “ y -phase” attractor and climbs towards maximal values of y . $\lambda = 0.5$, $D = 0.05$, $\sigma = 0.01$, $\Delta = 0$, $k_2 = 0.1$, $k_3 = 0.1$. Initial conditions: $x = 0$, $y = 0.4$, $z = 0$, $p = 0$ everywhere.

One can observe a synchronisation effect: the values of y , z and p decrease when x increase, and *vice versa* (see Figs. 10, 12). One can also notice the stabilising effect of diffusion. Fig. 8 compares trajectories of two systems: with and without diffusion, driven by additive Gaussian noise. Without diffusion, the trajectory wanders up and down along the branch of stationary points. The trajectory stabilised by diffusion stays longer in the neighbourhood of its initial plane E .

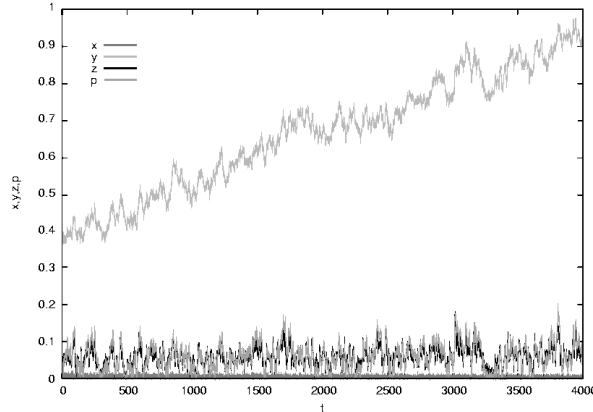


Fig. 12. The time-evolution of x, y, z and p . in the system with additive Gaussian noise and diffusion, recorded at point $[20, 20]$ on the spatial lattice. $K_1 = k_1 + \Delta = 2.25$, $\lambda = 0.5$, $D = 0.05$, $\sigma = 0.01$, $\Delta = 0$, $k_2 = 0.1$, $k_3 = 0.1$. Initial conditions as above.

4.6. System with Gaussian noise, dichotomous noise and diffusion

The system (4) is a combination of all cases analysed above. Dichotomous noise switches the system between states where either the “ x -phase” or the “ y -phase” is preferred. This causes the emergence of separate “islands” of these two phases. Their boundaries move due to diffusion and the direction and speed of the motion depends on the current value of $k_1 + \eta(t)$ (see Figs. 1, 15). In the x - y - z -space, the trajectories climb up towards the region where y is close to 1 (the upper part of the y -phase attractor). This “climbing” effect is caused by the boundary conditions imposed on the system: Since the same positive or negative value of $\sigma\xi(\vec{r}, t)$ is being added to each equation, there is a certain preferred direction in which the trajectory moves. It cannot, however, cross the boundaries and thus, near the attracting branch of (7), the average direction of motion is “upwards” (*i.e.* towards the increasing values of y) because the motion in the opposite direction is blocked due to the boundary conditions (see Fig. 14).

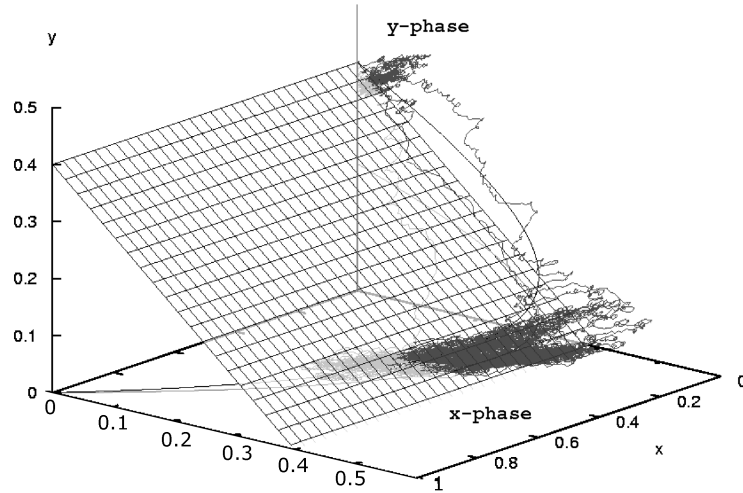


Fig. 13. Trajectory of the system (4) recorded at point $[20, 20]$ on the spatial lattice. Simulation time $T = 4000$. The trajectory jumps between two possible phases. Initial conditions: $x = 0$, $y = 0.4$, $z = 0$, $p = 0$ everywhere. Parameters: $\lambda = 0.5$, $D = 0.05$, $\sigma = 0.01$, $\Delta = 0.5$, $k_1 = 1.75$, $k_2 = 0.1$, $k_3 = 0.1$, $\gamma = 0.01$.

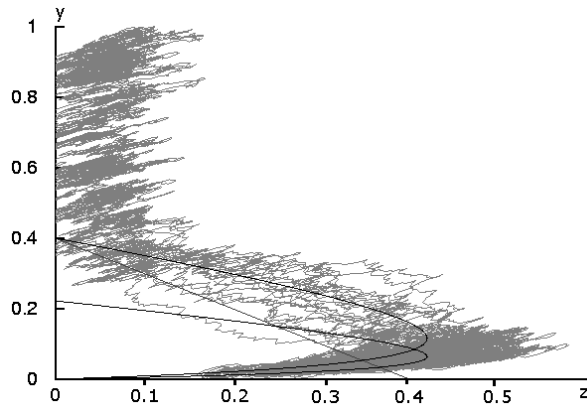


Fig. 14. Trajectory of the system (4) recorded at point $[20, 20]$ on the spatial lattice, y - z -projection, simulation time $T = 10000$. The trajectory jumps between two stable branches of stationary points, but, finally, it climbs up the “ y -phase” branch. Initial conditions: $x = 0$, $y = 0.4$, $z = 0$, $p = 0$ everywhere. Parameters: $\lambda = 0.5$, $D = 0.05$, $\sigma = 0.01$, $\Delta = 0.5$, $k_1 = 1.75$, $k_2 = 0.1$, $k_3 = 0.1$, $\gamma = 0.01$. Curves show how the shape of branches of stationary points changes with switching value of $k_1 \pm \Delta$. Sloped line: the initial plane $E = 0.4$.

When trajectories get to the upper part of the “*y*-phase” attractor, they remain in its neighbourhood for all time because the “*x*-phase” attractor is too distant. This distance is determined by the choice of parameters, namely by the position of point $\{0, \frac{\lambda}{k_1}, 0, 0\}$ where the other branch of stationary points begins (see Fig. 14). This effect is the reason why the “*y*-phase” finally spreads all over accessible space in our simulation.

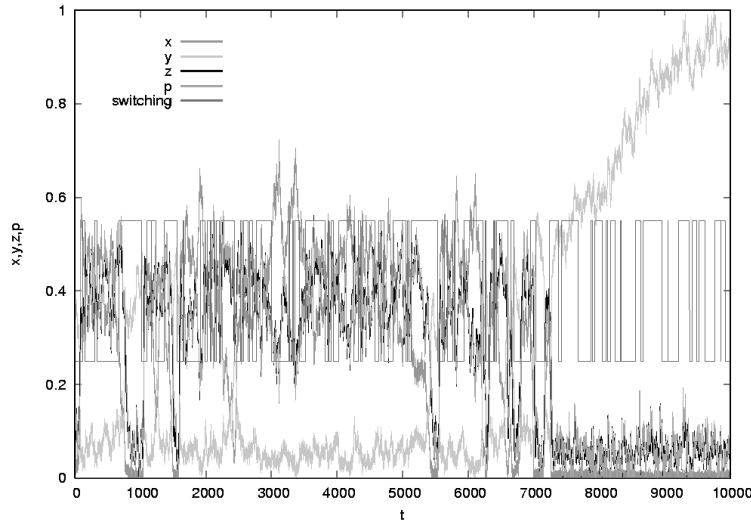


Fig. 15. Time evolution of x, y, z and p in system (4). Simulation time $T = 10000$. Initial conditions: $x = 0, y = 0.4, z = 0, p = 0$ everywhere. Parameters: $\lambda = 0.5, D = 0.05, \sigma = 0.01, \Delta = 0.5, k_1 = 1.75, k_2 = 0.1, k_3 = 0.1, \gamma = 0.01$.

5. Conclusions

We have performed a simulation of a spatially inhomogeneous model of cancer growth with additive Gaussian noise and multiplicative dichotomous noise. The multiplicative noise controls the efficiency of the immune response whereas the external environmental fluctuations have been modelled by the additive Gaussian noise.

The presence of noise in biological systems may be regarded not only as a mere source of disorder but also as a factor which introduces positive and organising rather than disruptive changes in the system’s dynamics: In our model, we find that the presence of a global (*i.e.* depending only on time) multiplicative dichotomous noise in a system perturbed by a spatially inhomogeneous additive Gaussian noise leads to emergence of a spatial pattern of two “phases”. The “phases” are distinct areas in which cancer cells, or,

respectively, immune cells predominate. The pattern is not stable: domain boundaries move due to a diffusion effect, and the direction (and speed) of that motion is determined by the current value of the dichotomous noise, *i.e.* by the effective intensity of the immune response.

The spatial pattern emerges when the environmental noise intensity σ is properly tuned. Combined with the multiplicative noise, it should allow the system to perform transitions between two “phases”. Too strong additive noise would however dominate the picture, preventing the formation of a pattern. Additionally, the diffusion parameter D should be carefully chosen, so that the pattern could have sufficiently distinct boundaries and be relatively stable. If the diffusion rate is high, the pattern dissolves quickly, whereas at small diffusion rate it only forms small “grains”. The quantitative analysis of the interplay between the above-mentioned factors in the process of pattern formation [21] merits a further study.

After a sufficiently long time, the immune cells prevail globally. This turns out to be the effect of reflecting boundary conditions, which prevent the population densities from exceeding 0 or 1. The existence of such boundaries causes that the trajectories of the system prefer to move in the direction of greater population of immune cells. A replacement of the additive Gaussian noise $\xi(\vec{r}, t)$ with a multiplicative Gaussian noise, and a comparison with the model described here, would be another interesting issue for future research.

The author would like to thank Dr. Ewa Gudowska-Nowak for helpful discussions and comments.

REFERENCES

- [1] J.D. Murray: *Mathematical Biology*, Springer-Verlag, Berlin 1993.
- [2] B. Spagnolo, D. Valenti, A. Fiasconaro, *Noise in Ecosystems: A Short Review, Mathematical Biosciences and Engineering 1*, in press, [arXiv:q-bio.PE/0403004](https://arxiv.org/abs/q-bio.PE/0403004).
- [3] R.K. Sachs, L.R. Hlatky, P. Hahnfeld, *Math. Comp. Modelling* **33**, 1297 (2001).
- [4] P. Hahnfeld, R.K. Sachs, In: *Advances in Mathematical Population Dynamics: Molecules, Cells and Man*, Edited by O. Arino, D. Axelrod, M. Kimmel, World Scientific Publishing Company, 1998.
- [5] L. Gammaitoni, P. Hänggi, P. Jung, F. Marchesoni, *Rev. Mod. Phys.* **70**, 223 (1998).
- [6] C.R. Doering, J.C. Gadoua, *Phys. Rev. Lett.* **69**, 2318 (1992).
- [7] J. Iwaniszewski, *Phys. Rev.* **E68**, 027105 (2003).
- [8] A. Ochab-Marcinek, E. Gudowska-Nowak, *Physica A* **343**, 557 (2004).

- [9] W. Horsthemke, R. Lefever: *Noise-Induced Transitions. Theory and Applications in Physics, Chemistry and Biology*, Springer-Verlag, Berlin 1984.
- [10] C. Van den Broeck, J.M.R. Parrondo, R. Torral, *Phys. Rev. Lett.* **73**, 3395 (1994).
- [11] B. Spagnolo, A.A. Dubkov, N.V. Agudov, *Eur. Phys. J.* **B40**, 273 (2004).
- [12] D. Valenti, A. Fiasconaro, B. Spagnolo, *Acta Phys. Pol. B* **35**, 1481 (2004).
- [13] R.P. Garay, R. Lefever, *J. Theor. Biol.* **73**, 417 (1978).
- [14] N. Stepanova, *Biophysics* **24**, 917 (1980).
- [15] H.P. Vlardar, J.A. Gonzalez, *J. Theor. Biol.* **227**, 335 (2004).
- [16] I. Prigogine, R. Lefever, *Comput. Biochem. Physiol.* **67B**, 389 (1980).
- [17] R. Lefever, W. Horsthemke, *Bulletin of Mathematical Biology* **41**, 469 (1978).
- [18] J.C.M. Mombach, N. Lemke, B.E.J. Bodmann, M.A.P. Idiart, *Europhys. Lett.* **56**(6), 923 (2002).
- [19] R. Garay, R. Lefever, *Local Description of Immune Tumor Rejection, Developments in Cell Biology* **2**, *Biomathematics and Cell Kinetics* (1978).
- [20] P.C. Fife, *J. Chem. Phys.* **64** (2), (1976).
- [21] A. Fiasconaro, D. Valenti, B. Spagnolo, *Acta Phys. Pol. B* **35**, 1491 (2004).